Clinical Oncology 35 (2023) e10–e19

Contents lists available at ScienceDirect

Clinical Oncology

journal homepage: www.clinicaloncologyonline.net

Original Article

A New Approach to Quantify and Grade Radiation Dermatitis Using Deep-Learning Segmentation in Skin Photographs

Y.I. Park *‡, S.H. Choi *†, C.-S. Hong *, M.-S. Cho †, J. Son †, M.C. Han *, J. Kim *, H. Kim *, D.W. Kim *, J.S. Kim *‡

* Department of Radiation Oncology, Yonsei University College of Medicine, Seoul, South Korea
† Department of Radiation Oncology, Yongin Severance Hospital, Yongin, South Korea
‡ Medical Physics and Biomedical Engineering Lab (MPBEL), Yonsei University College of Medicine, Seoul, South Korea

Abstract

Aims: Objective evaluation of radiation dermatitis is important for analysing the correlation between the severity of radiation dermatitis and dose distribution in clinical practice and for reliable reporting in clinical trials. We developed a novel radiation dermatitis segmentation system based on convolutional neural networks (CNNs) to consistently evaluate radiation dermatitis.

Materials and methods: The radiation dermatitis segmentation system is designed to segment the radiation dermatitis occurrence area using skin photographs and skin-dose distribution. A CNN architecture with a dilated convolution layer and skip connection was designed to estimate the radiation dermatitis area. Seventy-three skin photographs obtained from patients undergoing radiotherapy were collected for training and testing. The ground truth of radiation dermatitis segmentation is manually delineated from the skin photograph by an experienced radiation oncologist and medical physicist. We converted the skin photographs to RGB (red-green-blue) and CIELAB (lightness (L^*), red-green (a^*) and blue-yellow (b^*)) colour information and trained the network to segment faint and severe radiation dermatitis using three different input combinations: RGB, RGB + CIELAB (RGBLAB) and RGB + CIELAB + skin-dose distribution (RGBLAB_D). The proposed system was evaluated using the Dice similarity coefficient (DSC), sensitivity, specificity and normalised Matthews correlation coefficient (nMCC). A paired *t*-test was used to compare the results of different segmentation performances.

Results: Optimal data composition was observed in the network trained for radiation dermatitis segmentation using skin photographs and skin-dose distribution. The average DSC, sensitivity, specificity and nMCC values of RGBLAB_D were 0.62, 0.61, 0.91 and 0.77, respectively, in faint radiation dermatitis, and 0.69, 0.78, 0.96 and 0.83, respectively, in severe radiation dermatitis.

Conclusion: Our study showed that CNN-based radiation dermatitis segmentation in skin photographs of patients undergoing radiotherapy can describe radiation dermatitis severity and pattern. Our study could aid in objectifying the radiation dermatitis grading and analysing the reliable correlation between dosimetric factors and the morphology of radiation dermatitis.

Key words: Convolutional neural networks; dermatitis grading scale; radiation dermatitis; radiation therapy; skin toxicity; skin-dose distribution

Introduction

Radiation dermatitis is a common side-effect of radiotherapy manifested through skin changes, such as erythema, desquamation and ulceration; about 90% of patients receiving radiotherapy experience acute radiation dermatitis [1,2]. Skin toxicities induced by radiation include cosmetic change, pain, discomfort and risk of infection, which decrease the quality of life after radiotherapy. Moreover, severe radiation dermatitis can lead to interruption or premature discontinuation of radiotherapy and have a potentially negative impact on treatment outcomes [3–5]. Therefore, establishing an accurate correlation between the dose distribution and the incidence, as well as the severity, of radiation dermatitis is important in clinical practice and for reliable and valid reporting in clinical trials.

The severity of radiation dermatitis is assessed based on simple grading systems, such as Radiation Therapy Oncology Group (RTOG) and Common Terminology Criteria for Adverse Effects (CTCAE) [6,7]. RTOG and CTCAE classify

Authors for correspondence: Chae-Seon Hong, Department of Radiation Oncology, Yonsei Cancer Center, Yonsei University College of Medicine, 50-1 Yonsei-ro, Seodaemun-gu, Seoul 03722, South Korea.
Authors for correspondence: Jin Sung Kim, Department of Radiation Oncology, Yonsei Cancer Center, Yonsei University College of Medicine, 50-1 Yonsei-ro, Seodaemun-gu, Seoul 03722, South Korea.
E-mail addresses: cs.hong@yuhs.ac (C.-S. Hong), JINSUNG@yuhs.ac (J.S. Kim).

https://doi.org/10.1016/j.clon.2022.07.001

the degree of radiation dermatitis from faint to severe by observing skin changes induced due to irradiation, such as pigmentation, erythema, desquamation, ulceration and necrosis. Grading through visual inspection of radiation dermatitis is a common method of evaluating radiation dermatitis. However, this method entails a risk of subjective interpretation by individual evaluators.

Various methods have been proposed to reduce the variability in radiation dermatitis grading through visual inspection. Creating and utilising a radiation dermatitis grading atlas by collecting radiation dermatitis photographs can make radiation dermatitis grading more consistent [8,9]. However, the accuracy and reliability of radiation dermatitis grading may be compromised because of subjective interpretations through visual inspection by individual evaluators.

Skin photographs obtained from patients who underwent radiotherapy are an important factor in objectifying the radiation dermatitis grading based on visual inspection. Colorimetric features, such as RGB (red-green-blue) and CIELAB (lightness (L^*), red-green (a^*) and blue-yellow (b^*)), are important factors in identifying erythema and pigmentation in skin photographs [10–13]. Accordingly, researchers have attempted to quantify the grading process of radiation dermatitis based on the colour features in skin photographs in recent years [14–16]. An efficient and objective radiation dermatitis grading system is lacking despite the efforts to quantify the scoring system for severe radiation dermatitis. The radiation dermatitis grade obtained based on the colour features in skin photographs is expressed as a single numeric number that cannot contain information about the heterogeneity in the severity of radiation dermatitis in a patient [12,17]. Moreover, various dosimetric indices represent the important risk factors associated with the severity of radiation dermatitis [4,18–21]. However, the correlation between skin-dose distribution and radiation dermatitis based on morphology has not been established. Thus, the shape of radiation dermatitis should be described quantitatively in addition to the objectification of radiation dermatitis grading to establish the correlation between the spatial distribution of dosimetric factors and radiation dermatitis.

The aim of this study was to develop a radiation dermatitis segmentation system using a convolutional neural network (CNN) in skin photographs of patients undergoing radiotherapy. To the best of our knowledge, we are the first to attempt the segmentation of the occurrence and morphology of radiation dermatitis in the photographs of patients based on severity. The proposed deep-learning segmentation system segments and identifies the area of radiation dermatitis into two different levels (from faint to severe) based on the CTCAE grading system, using patient skin photographs and skin-dose distribution. Our study demonstrates the application of radiation dermatitis segmentation as a new scale for objectively grading and classifying radiation dermatitis with heterogeneity in the irradiated area of patient's skin. Furthermore, the quantification of the radiation dermatitis occurrence area makes it possible to determine the skin-dose distribution that directly coincides with the area afflicted by radiation dermatitis. This can be a major step in determining the normal tissue complication probability (NTCP) based on skin-dose distribution.

Materials and Methods

The radiation dermatitis segmentation system is illustrated in Figure 1. In our study, the proposed CNN was trained to segment radiation dermatitis into two different labels: faint radiation dermatitis (CTCAE = 1) and severe radiation dermatitis (CTCAE $\geq$ 2). The dataset for developing the proposed system consists of colorimetric and dosimetric features obtained from skin photography and treatment planning data, respectively, of patients who have received radiotherapy. The colorimetric features were extracted from skin photographs to RGB and CIELAB to provide detailed information of skin photographs to CNN. Treatment planning data were used to generate skin-dose distribution maps representing the spatial information of skin dose. The collected dataset was preprocessed to standardise the shape of the training dataset. The preprocessed dataset was split into training and test data via stratified random sampling to maintain the balance between radiation dermatitis labels. The performance of the developed system was evaluated after training using combinations of three different input data: RGB, RGB + CIELAB and RGB + CIELAB + skin-dose distribution.

Data Acquisition and Preprocessing

We retrospectively collected skin photographs of patients who underwent radiotherapy at our institute between September 2020 and February 2021. These included head and neck, breast and thoracic cancer patients. Patients were treated with either volumetric-modulated radiotherapy or three-dimensional conformal radiotherapy. The prescribed doses of the radiotherapy ranged from 28.8 to 70 Gy in 15–33 fractions. All patients were given daily fractions of 2–3 Gy. This study was approved by the institutional review board at the Yongin Severance Hospital, and all procedures were carried out in accordance with relevant guidelines and regulations. Our study was based on a review of retrospective charts of patients who developed radiation dermatitis due to radiotherapy. An informed consent waiver was obtained from Yongin Severance Hospital (9-2020-0163) because of the retrospective nature of the study and the use of anonymised data.

Photographs of skin affected by radiation dermatitis were obtained using a three-dimensional camera (Intel RealSense Depth Camera D435i, Intel, Santa Clara, CA, USA) that could simultaneously scan colour and depth information [22]. The radiation dermatitis was segmented into two different labels to evaluate the shape and severity of radiation dermatitis symptoms based on the CTCAE scoring result: faint (grade 1) and severe ($\geq$grade 2) symptoms.

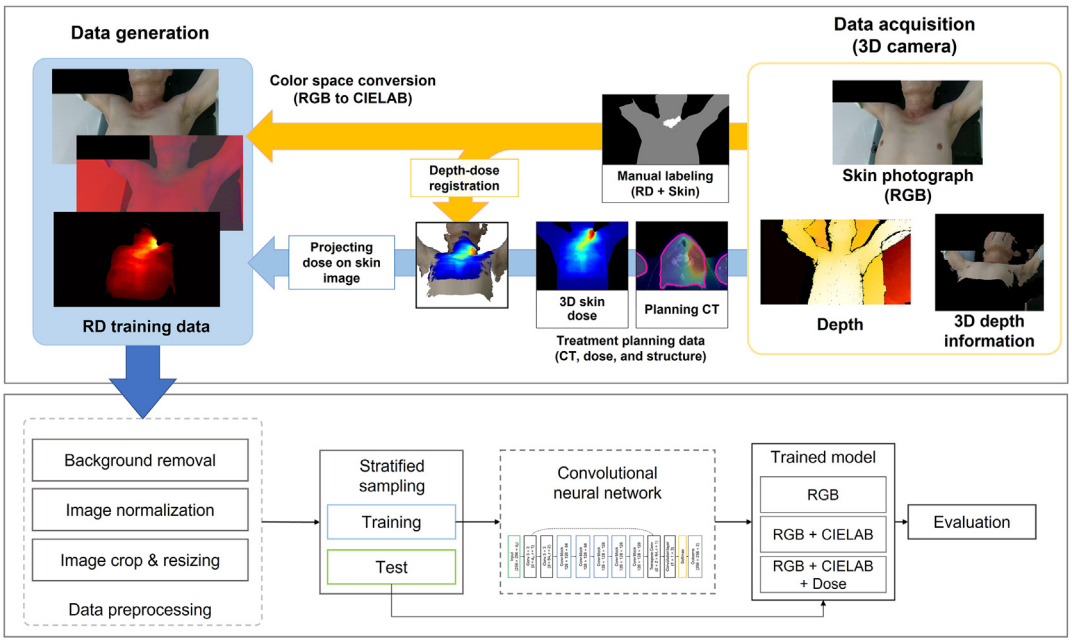

Fig 1. Schematic diagram of the proposed model. The skin photograph and skin-dose distribution map are used to develop the radiation dermatitis segmentation system. The ground truth of radiation dermatitis segmentation is manually delineated from the skin photograph by an experienced radiation oncologist and medical physicists. The skin-dose distribution is registered with skin surface data obtained from a three-dimensional camera and converted into a two-dimensional image. The skin background region in the radiation dermatitis training data is removed based on labels of normal skin followed by image preprocessing. The proposed convolutional neural network for segmenting radiation dermatitis is trained using three different radiation dermatitis training input datasets.

Radiation dermatitis was delineated manually by an experienced radiation oncologist and medical physicists with the assistance of a graph-cut algorithm implemented in the MATLAB Image Segmenter. Visual changes due to the development of patch moist desquamation are the main criterion for defining the severe radiation dermatitis label. Skin photographs obtained from the radiotherapy patients who did not develop radiation dermatitis at data acquisition (CTCAE grade 0) were included in the dataset as no-label images.

Radiation dermatitis skin photographs were used in two different colour spaces, RGB and CIELAB, in our study based on the analysis of the significant correlation between L^*, a^*, and b^* values and the severity of radiation dermatitis in past studies [14,15,23]. Skin photographs are captured in the RGB colour space with an 8-bit range of [0,255] and converted into the 1976 CIELAB colour space [24]. The pixel values of L^*, a^* and b^* maps are represented as [0,100], [−128,127] and [−128,127] ranges, respectively.

A skin-dose distribution map was generated based on the treatment planning file and used as a supplementary input in the CNN for radiation dermatitis segmentation. The final dose distribution was calculated by a collapsed cone convolution algorithm (RaySearch Laboratories AB, Stockholm, Sweden) with a dose grid of 2 mm × 2 mm × 2 mm. We obtained the dose distribution from 2 mm under the external body contour using the calculated dose of the treatment planning system (TPS) and radiotherapy structure set file. The three-dimensional skin-dose distribution obtained from the external body contour was converted into a point cloud array consisting of the position and intensity values of the dose pixels. The skin depth information of the region of interest was extracted from the patient's skin photograph obtained with a three-dimensional camera. The surface registration between the skin-dose distribution and the patient skin photograph was carried out using the iterative closest point algorithm under the tolerance condition of 0.5 mm and with a maximum of 1000 iterations. The point-to-point iterative closest point algorithm provided by MATLAB Version 2020b was used for surface registration. Then, the dose distribution corresponding to the skin depth information was projected onto the plane of the two-dimensional depth image to match the skin area of the RGB photographs. A ray-tracing algorithm was applied to two-dimensional projection based on the intrinsic matrix of the three-dimensional camera [25].

Data preprocessing included background removal, normalisation and image cropping. Background removal was carried out to prevent CNNs from training non-skin areas such as clothes, band-aids and immobilisation devices. The background region was delineated manually and its pixel values were set to zero in both colour and dose images. The colour maps of the skin photography were normalised from the full range of each colour space: [0,255] for RGB, [0,100] for L^* and [−128,128] for a^*b^* to the range [0,1] after background removal. Moreover, the pixel values of the skin-dose distribution map were converted into the equivalent doses in 2 Gy fractions (EQD2) with an α/β of 10 Gy [26] to correct for the difference in fractionation regimen. The converted skin dose was truncated into a prescription dose range of

5–60 Gy and divided by 60 Gy to normalise the values in the interval [0,1]. The normalised dose (D) map was converted to accumulated dose (AD) up to the time of skin photograph acquisition according to the equation, $AD = D \times N_{Delivered}/N_{Total}$. Here, D is the normalised dose; $N_{Delivered}$ and N_{Total} are the number of delivered and total fractions, respectively. All radiation dermatitis data were cropped to 256 × 256 pixels and concatenated as multiple input channels for training the CNN. The number of trainable parameters of the proposed CNN are described in Supplementary Table S1.

CNN for Radiation Dermatitis Segmentation

We developed a two-dimensional CNN architecture to train the radiation dermatitis dataset, as shown in Figure 2. This work was inspired by the DeepLab-v3 with atrous spatial pyramid pooling [27]. The first layer calculated the 3 × 3 convolutions with the same number of filters as the input channels. The output of the first layer was downscaled by one-quarter using the 3 × 3 convolutions with stride 2, and it was passed through several convolution blocks, followed by batch normalisation and a rectified linear unit. Our network included five convolution blocks consisting of three parallel 3 × 3 convolution layers with the same filter size but different dilated factors, from one to three, for training radiation dermatitis features from various field sizes. The output features of the convolution layers were concatenated and then refined using a 1 × 1 convolution layer in each block. After the convolution blocks, feature upsampling was carried out via 2 × 2 transpose convolution to restore the image resolution to that of the input. Softmax activation was applied as the last layer of the model after reducing the channel size into 3 by utilising 1 × 1 convolution. The model detected the pixel that was classified as faint radiation dermatitis and severe radiation dermatitis using pixel-wise probability from three output channels. We carried out the conditional random field [28] operation for post-processing the network output to refine the segmentation output using contextual information between labels. The use of conditional random fields could eliminate small incorrect labels and smooth label outlines (Supplementary Figure S1). Some features in the network were copied and reused through the skip connection shown in Figure 2 to improve the performance of the network within a limited number of extracted features.

Network Training

The dataset used in the study included 73 skin photographs, comprising 37 faint radiation dermatitis (50.7%), 29 severe radiation dermatitis (39.7%) and seven no-label (9.6%) images. The dataset was divided into training and test datasets with a ratio of 6:4 using the stratified random sampling method based on the presence of faint/severe

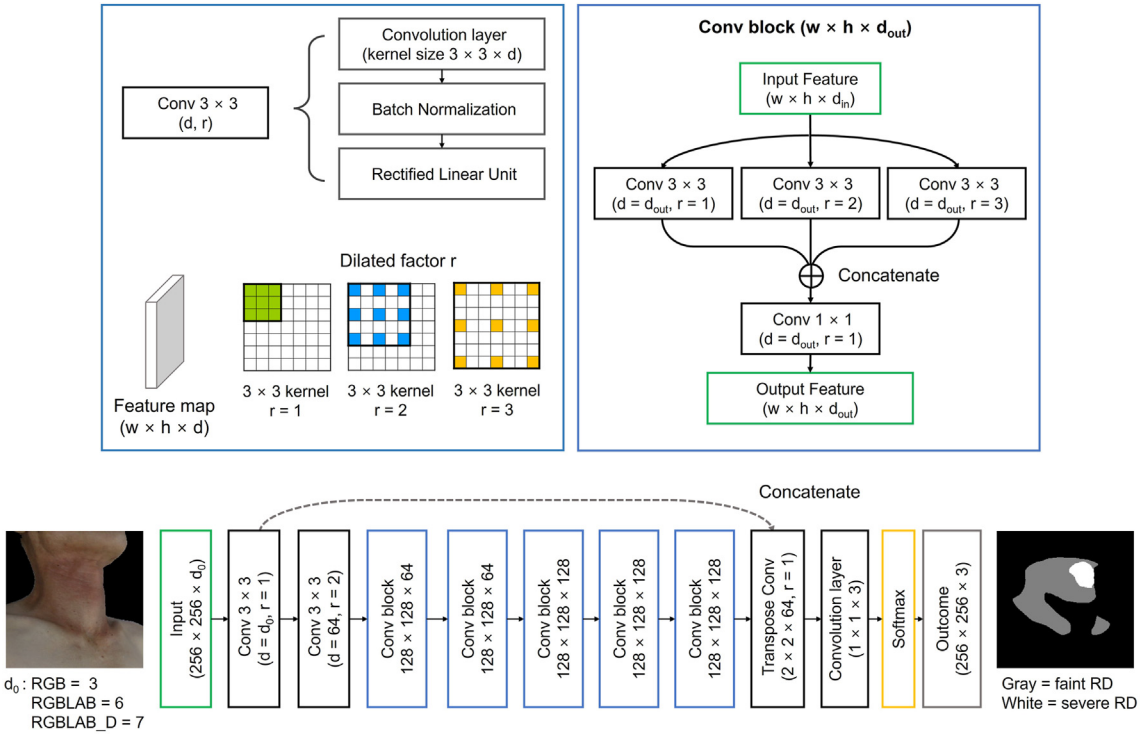

Fig 2. Architecture of the proposed convolutional neural network. The d value represents the depth of the feature map and input depth d_0 is the number of input channels for three different networks, RGB, RGBLAB and RGBLAB_D. The convolution block consisted of three 3 × 3 dilated convolution layers with a distinct dilated factor r. All 3 × 3 and 1 × 1 convolutions were followed by batch normalisation and rectified linear unit. The last 1 × 1 convolution layer reduced the depth of the feature map into three channels for network output and activated using Softmax without the batch normalisation and rectified linear unit. RGB, red-green-blue colour space; RGBLAB, RGB + CIELAB (CIELAB dimensions of lightness (L^*), red-green (a^*) and blue-yellow (b^*)); RGBLAB_D, RGB + CIELAB + skin-dose distribution.

radiation dermatitis. The training dataset consisted of 23 faint radiation dermatitis, 29 severe radiation dermatitis and four no-label images; we carried out data augmentation techniques to avoid network overfitting due to small datasets. We carried out random rotation from 0 to 20 degrees and vertical or horizontal flips on the dataset during network training.

Our network was trained with three combinations of input data: RGB (three channels), RGB + CIELAB (RGBLAB, six channels) and RGB + CIELAB + skin-dose (RGBLAB_D, seven channels). The first 3×3 convolution layer possessed the optimal filter size that could be adjusted to fit the input channels 3, 6 and 7. The number of trainable parameters in each input condition is summarised in Supplementary Table S1. Network training was conducted using 10-fold cross-validation for the training dataset to generalise the performance of the networks trained on the small dataset. The generalised Dice loss [29] was used as an objective function for network training with multi-class output and was minimised using the Adam optimiser [30] with an initial learning rate of 1e-4. All networks were trained up to 200 epochs with early stopping to avoid overfitting. The network architecture was implemented using PyTorch library version 1.6.0 (Cuda 10.1) on NVIDIA RTX 2060 GPU.

Evaluation Metrics

The performance of the proposed three networks was evaluated in terms of the Dice similarity coefficient (DSC), sensitivity, specificity and normalised Matthews correlation coefficient (nMCC). The values of the three metrics were computed using the pixel-based confusion matrix with the following equations, where a value of one indicates a perfect overlap between ground truth and network output:

$$DSC = \frac{2 \times TP}{2 \times TP + FP + FN} \quad (1)$$

$$Sensitivity = \frac{TP}{TP + FN} \quad (2)$$

$$Specificity = \frac{TN}{TN + FP} \quad (3)$$

$$nMCC = \frac{1}{2}(1 + MCC) = \frac{1}{2}\left(1 + \frac{TP \times TN - FP \times FN}{\sqrt{(TP + FP)(TP + FN)(TN + FP)(TN + FN)}}\right) \quad (4)$$

where true positive (TP) and true negative (TN) are the numbers of pixels correctly diagnosed as positive and negative, respectively, and false positive (FP) and false negative (FN) are the number of pixels incorrectly diagnosed as positive and negative, respectively (see Supplementary Table S2). The confusion matrix was calculated for pixels located within the patient skin area and network performance was evaluated for segmentation labels of faint and severe radiation dermatitis. A paired *t*-test was used to compare the segmentation performance difference of DSC, sensitivity, specificity and nMCC. Statistical significance was defined as $P < 0.05$.

Results

The DSC, sensitivity, specificity and nMCC values were calculated for the faint and severe radiation dermatitis labels, the results for which are summarised in Tables 1 and 2. The network was tested using 28 images, comprising 14 faint radiation dermatitis, 11 severe radiation dermatitis and three no-label. The average DSC, sensitivity, specificity and nMCC values of the RGBLAB_D network (i.e. 0.62, 0.61, 0.91 and 0.77, respectively) were higher than those of the RGB (i.e. 0.50, 0.56, 0.85 and 0.70, respectively) and the RGBLAB (i.e. 0.52, 0.60, 0.84 and 0.70, respectively) networks in the faint radiation dermatitis segmentation. Moreover, in the severe radiation dermatitis segmentation, the average DSC, sensitivity, specificity and nMCC values of the RGBLAB_D (i.e. 0.69, 0.78, 0.96 and 0.83, respectively) network were higher than those of the RGB (i.e. 0.40, 0.41, 0.94 and 0.70, respectively) and RGBLAB (i.e. 0.44, 0.39, 0.96 and 0.72, respectively) networks. The RGBLAB_D network showed a statistically significant difference in DSC and nMCC than other networks in both faint and severe radiation dermatitis segmentation and achieved the best performance in severe radiation dermatitis segmentation ($P < 0.001$). The RGBLAB network showed a similar or improved performance in faint and severe radiation dermatitis segmentation compared with RGB. Representative images of radiation dermatitis segmentation for three different networks are presented in Figure 3. The confusion matrix calculated for the model evaluation was normalised by the number of pixels in the ground truth label, as illustrated in Figure 4.

Discussion

This study aimed to develop an image-based radiation dermatitis assessment system using CNN. The primary strength of our study was that radiation dermatitis can be objectively graded and heterogeneous radiation dermatitis can be evaluated in terms of morphology by segmenting the radiation dermatitis occurrence area based on severity using skin photographs of patients who have received radiotherapy. Hence, we can improve the reliability and validity of radiation dermatitis grading and explain the correlation between skin-dose distribution and the occurrence of

Table 1
Comparison of segmentation performance of the trained networks on faint and severe radiation dermatitis

Networks	Faint radiation dermatitis (CTCAE grade = 1)				Severe radiation dermatitis (CTCAE grade ≥ 2)			
	DSC	Se	Sp	nMCC	DSC	Se	Sp	nMCC
RGB	0.50 ± 0.21	0.56 ± 0.25	0.85 ± 0.13	0.70 ± 0.11	0.40 ± 0.22	0.41 ± 0.29	0.94 ± 0.06	0.70 ± 0.11
RGBLAB	0.52 ± 0.22	0.60 ± 0.27	0.84 ± 0.14	0.70 ± 0.13	0.44 ± 0.24	0.39 ± 0.26	**0.96 ± 0.04**	0.72 ± 0.11
RGBLAB_D	**0.62 ± 0.21**	**0.61 ± 0.25**	**0.91 ± 0.12**	**0.77 ± 0.11**	**0.69 ± 0.21**	**0.78 ± 0.28**	**0.96 ± 0.04**	**0.83 ± 0.10**

CTCAE, Common Terminology Criteria for Adverse Effects; DSC, Dice similarity coefficient; nMCC, normalised Matthews correlation coefficient; RGB, red-green-blue colour space; RGBLAB, RGB + CIELAB (CIELAB dimensions of lightness (L^*), red-green (a^*) and blue-yellow (b^*) values); RGBLAB_D, RGB + CIELAB + skin-dose distribution; Se, sensitivity; Sp, specificity.
All values are represented as mean ± standard deviation and the best results are highlighted in bold.

Table 2
P values for the comparison of different segmentation methods

Networks	Faint radiation dermatitis (CTCAE grade = 1)				Severe radiation dermatitis (CTCAE grade ≥ 2)			
	DSC	Se	Sp	nMCC	DSC	Se	Sp	nMCC
RGB versus RGBLAB	0.33	**0.003**	0.22	0.69	**<0.001**	0.30	0.07	0.28
RGB versus RGBLAB_D	**<0.001**	**<0.001**	**<0.001**	**<0.001**	**<0.001**	**<0.001**	0.06	**<0.001**
RGBLAB versus RGBLAB_D	**<0.001**	0.78	**<0.001**	**<0.001**	**<0.001**	**<0.001**	0.71	**<0.001**

CTCAE, Common Terminology Criteria for Adverse Effects; DSC, Dice similarity coefficient; nMCC, normalised Matthews correlation coefficient; RGB, red-green-blue colour space; RGBLAB, RGB + CIELAB (CIELAB dimensions of lightness (L^*), red-green (a^*) and blue-yellow (b^*) values); RGBLAB_D, RGB + CIELAB + skin-dose distribution; Se, sensitivity; Sp, specificity.
Statistically significant results ($P < 0.05$) are highlighted in bold.

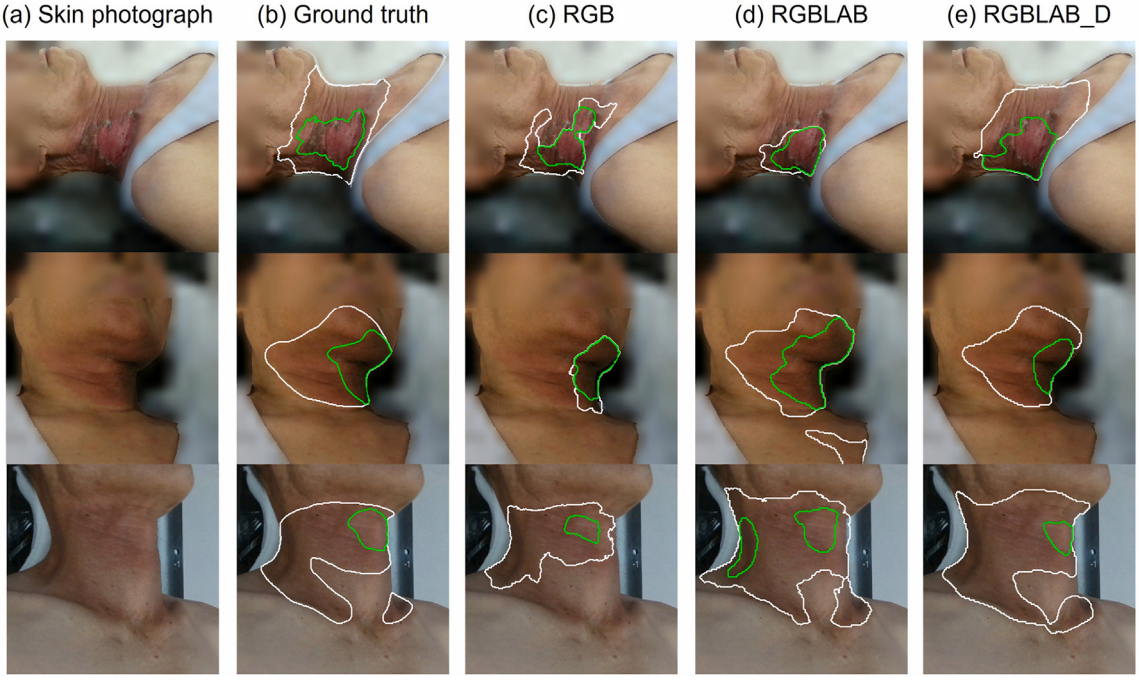

Fig 3. Representative images of radiation dermatitis segmentation. (a) Input data (skin photograph), (b) ground truth of radiation dermatitis segmentation, (c)–(e) segmentation output of RGB, RGBLAB and RGBLAB_D. The white contour denotes faint radiation dermatitis (CTCAE grade = 1) and green contours denote severe radiation dermatitis (CTCAE grade ≥ 2). RGB, red-green-blue colour space; RGBLAB, RGB + CIELAB (CIELAB dimensions of lightness (L^*), red-green (a^*) and blue-yellow (b^*)); RGBLAB_D, RGB + CIELAB + skin-dose distribution.

radiation dermatitis. Our findings demonstrate that the RGBLAB_D network can delineate both faint and severe radiation dermatitis based on skin photographic images. To the best of our knowledge, this is the first study to assess the severity and distribution of radiation dermatitis simultaneously for grading radiation dermatitis.

Some previous researchers have used quantitative approaches using corneometry, Doppler flowmetry and

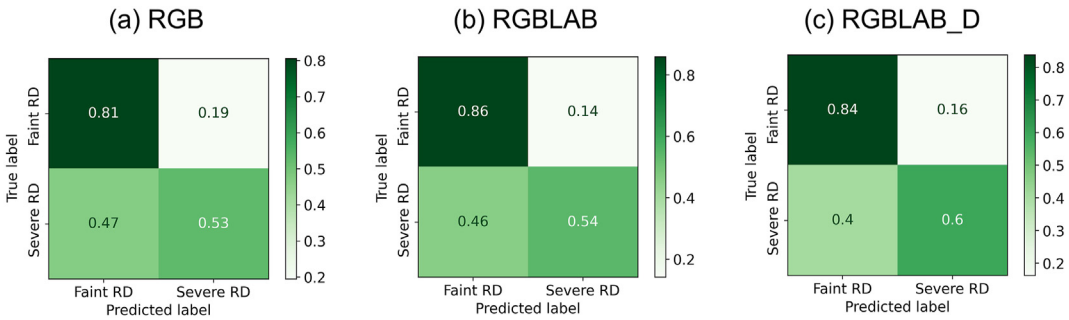

Fig 4. Confusion matrices of (a) RGB network, (b) RGBLAB network and (c) RGBLAB_D network. The numbers in squares are the pixel ratios classified to each label and normalised using the number of the true labels. RGB, red-green-blue colour space; RGBLAB, RGB + CIELAB (CIELAB dimensions of lightness (L^*), red-green (a^*) and blue-yellow (b^*) values); RGBLAB_D, RGB + CIELAB + skin-dose distribution.

spectrophotometry to provide an objective assessment of radiation dermatitis [31–35]. However, these methods need to overcome certain limitations to completely replace the conventional grading systems based on visual inspection. Most devices utilised for detecting skin changes have a small field of view. Therefore, these devices require a long time to measure the entire radiation dermatitis area. Moreover, a few devices require contact with the radiation dermatitis area, inflicting pain on patients during measurement. Therefore, photograph-based radiation dermatitis grading is preferred for assessing radiation dermatitis for daily treatment schedules in clinics. Hence, our approach of using skin photography for radiation dermatitis grading provides reproducible and objective scales for evaluating radiation dermatitis and easy applicability in clinical practice.

In our study, we used a CNN to segment two different areas based on faint or severe radiation dermatitis in skin photographs obtained from radiation dermatitis patients (Figure 3). We used skin photographs to quantify the radiation dermatitis grading systems because the change in skin colour is a major factor in radiation dermatitis grading. A study using CNNs to classify radiation dermatitis according to the CTCAE grading system has been reported recently [17,36]. However, CNNs were not used to segment the radiation dermatitis area from skin photographs of radiation dermatitis patients, based on severity. Moreover, the occurrence of radiation dermatitis was not assessed in terms of morphology and distribution, and radiation dermatitis with varying severities were still identified under a single numerical grade. The results of our study show that a CNN can be applied to develop a radiation dermatitis segmentation system based on skin photography (Table 1).

The DSC values of the RGBLAB network were greater than those of the RGB. This shows that using CIELAB colorimetry is beneficial for detecting the radiation dermatitis area. The L^*, a^*, and b^* ratios of skin photograph have been used to assess the severity of radiation dermatitis in past studies [10–12,23]. This is consistent with our observations that show improved segmentation using CIELAB colour information in the network input.

Skin-dose information is an important factor for improving the proposed radiation dermatitis segmentation system. We extracted the skin-dose distribution map from the calculated dose of the TPS and applied it for network training to analyse the relationship between skin dose and radiation dermatitis severity. Therefore, RGBLAB_D exhibited statistically significantly higher values in all evaluation metrics among the CNNs trained by three different datasets. Although skin-dose information is a relevant factor for radiation dermatitis segmentation, the skin-dose distribution consistent with the radiation dermatitis area may differ from patient to patient (see Supplementary Figure S2). Therefore, the radiation dermatitis segmentation performance can be improved when skin-dose distribution and colour features are used together. The radiation dermatitis-related skin-dose distribution map can be generated using a three-dimensional camera and treatment planning data. In a previous study, the mean deviation of the registration between the skin photograph and skin-dose distribution was within 0.3 mm on all axes [25].

Although various dosimetric factors have been used as predictive indicators of the incidence and severity of radiation dermatitis [4,20,21], the correlation between the shape of radiation dermatitis and the skin-dose distribution has not yet been studied. As the conventional radiation dermatitis grading system cannot describe the spatial distribution of radiation dermatitis severity, the correlation between dose distribution and the shape of radiation dermatitis could not be analysed. Therefore, assessing the morphology of radiation dermatitis development quantitatively is necessary. Our study can be used to evaluate skin toxicity in terms of morphology as well as objective grading of radiation dermatitis.

The segmentation of radiation dermatitis can impact future research on predicting skin tissue complications post-radiotherapy. The dose-response curve for an organ at risk is plotted using the NTCP model based on the single variable summarising the dose-volume histogram [37]. Recent studies have encouraged parameter optimisation for the NTCP model based on the differences in treatment technique and clinical environment [38,39]. However, NTCP optimisation using a single dosimetric variable may be less reliable in modern radiotherapy techniques, leading to inhomogeneous distribution of the degree of severity in the radiation dermatitis area [40,41]. The proposed system can provide detailed information about the shape of radiation dermatitis grading and skin-dose distribution. Hence, the

proposed system can be suitable for developing NTCP and other predictive models for radiation dermatitis with high reliability.

Our study had several limitations. First, the patients' skin photographs were taken in the treatment room under the same illuminance conditions, but may be under non-ideal illuminance conditions. Studies for developing photograph-based assessment systems have highlighted that image acquisition should be carefully carried out under normalised exposure conditions [17,42]. However, we obtained the skin photographs of radiation dermatitis patients without considering the environmental factors that affect image quality. Therefore, the segmentation performance of the proposed system can be increased by acquiring skin photographs under a controlled environment with constant illuminance, exposure and colour correction. Second, our findings were based on a limited number of radiation dermatitis photographs from a single institution. Data augmentation and early stopping were applied to reduce the risk of overfitting the model. We also generated CNN that are less complex than well-known architectures such as U-net [43,44]. This approach was effective for developing the radiation dermatitis segmentation model and showed similar performance with U-net trained using the fine-tuning technique (see Supplementary Table S3). Nevertheless, it still has the potential to overfit the model, or at least cause suboptimal weights. Moreover, we segmented the radiation dermatitis based on merely two grades, namely, faint and severe, because our dataset comprised small cases of radiation dermatitis that were insufficient for identifying the radiation dermatitis using the entire scale of traditional grading systems. Therefore, further research on large data from various patients is necessary for not only developing a comprehensive radiation dermatitis grading system but also for achieving the trade-off between the accuracy and the robustness of the model. Finally, although the use of three-dimensional cameras in radiotherapy treatment procedures, including surface-guided radiotherapy, has recently increased, the complexity of the method proposed in this study can potentially limit the use of this technique in clinical practice. Furthermore, the spatial accuracy of three-dimensional cameras and the registration accuracy of the skin-dose distribution may affect the performance of the CNN model, which has not been addressed in the current study.

Conclusions

We propose a radiation dermatitis segmentation system based on a deep-learning CNN. The results of our study showed that radiation dermatitis severity and pattern can be determined using skin photographs of patients undergoing radiotherapy. The use of skin-dose information can help increase the accuracy of the network for radiation dermatitis segmentation and assess the correlation between dose distribution and radiation dermatitis severity. Our proposed approach using severity and radiation dermatitis occurrence domain to objectify radiation dermatitis assessment improves the reliability and validity of the radiation dermatitis grading system. However, the results need to be interpreted with caution given the limitations of this study.

Conflicts of Interest

The authors declare no conflicts of interest.

Funding

This work was supported by the National Research Foundation of Korea (NRF) grant funded by the Korean Government (MSIT) (no. NRF-2020R1C1C1005713) and by a faculty research grant of Yonsei University College of Medicine (6-2021-0083).

Author Contributions

YP helped to design the software, reviewed the data and wrote the manuscript. SHC, MC and JS conceived the study design, provided input on data and algorithm analysis and wrote the manuscript. MCH, JK, HK and DK contributed to the data analysis and interpreted the results. JSK designed the analyses, interpreted the results, wrote the manuscript and supervised the project. CH designed the analyses, interpreted the results, wrote the manuscript, supervised and conceived the project.

Appendix A. Supplementary data

Supplementary data to this article can be found online at https://doi.org/10.1016/j.clon.2022.07.001.

References

[1] Lam E, Yee C, Wong G, Popovic M, Drost L, Pon K, *et al*. A systematic review and meta-analysis of clinician-reported versus patient-reported outcomes of radiation dermatitis. *Breast* 2020;50:125–134. https://doi.org/10.1016/j.breast.2019.09.009.

[2] Narvaez C, Doemer C, Idel C, Setter C, Olbrich D, Ujmajuridze Z, *et al*. Radiotherapy related skin toxicity (RAREST-01): Mepitel(R) film versus standard care in patients with locally advanced head-and-neck cancer. *BMC Cancer* 2018;18:197. https://doi.org/10.1186/s12885-018-4119-x.

[3] Bray FN, Simmons BJ, Wolfson AH, Nouri K. Acute and chronic cutaneous reactions to ionizing radiation therapy. *Dermatol Ther* 2016;6:185–206. https://doi.org/10.1007/s13555-016-0120-y.

[4] Mori M, Cattaneo GM, Dell'Oca I, Foti S, Calandrino R, Di Muzio NG, *et al*. Skin DVHs predict cutaneous toxicity in head and neck cancer patients treated with tomotherapy. *Phys Med* 2019;59:133–141. https://doi.org/10.1016/j.ejmp.2019.02.015.

[5] Giro C, Berger B, Bolke E, Ciernik IF, Duprez F, Locati L, *et al*. High rate of severe radiation dermatitis during radiation therapy with concurrent cetuximab in head and neck cancer: results of a survey in EORTC institutes. *Radiother Oncol* 2009;90:166–171. https://doi.org/10.1016/j.radonc.2008.09.007.

[6] Cox JD, Stetz J, Pajak TF. Toxicity criteria of the Radiation Therapy Oncology Group (RTOG) and the European Organization for Research and Treatment of Cancer (EORTC). *Int J Radiat Oncol Biol Phys* 1995;31:1341–1346. https://doi.org/10.1016/0360-3016(95)00060-C.

[7] Common Terminology Criteria for Adverse Events: (CTCAE) Ver 4.03. Available at: https://evs.nci.nih.gov/ftp1/CTCAE/CTCAE_4.03/CTCAE_4.03_2010-06-14_QuickReference_8.5x11.pdf 2010; 2010.

[8] Peuvrel L, Cassecuel J, Bernier C, Quereux G, Saint-Jean M, Le Moigne M, *et al*. TOXICAN: a guide for grading dermatological adverse events of cancer treatments. *Support Care Cancer* 2018;26:2871–2877. https://doi.org/10.1007/s00520-018-4153-x.

[9] Zenda S, Ota Y, Tachibana H, Ogawa H, Ishii S, Hashiguchi C, *et al*. A prospective picture collection study for a grading atlas of radiation dermatitis for clinical trials in head-and-neck cancer patients. *J Radiat Res* 2016;57:301–306. https://doi.org/10.1093/jrr/rrv092.

[10] Schmeel LC, Koch D, Schmeel FC, Rohner F, Schoroth F, Bucheler BM, *et al*. Acute radiation-induced skin toxicity in hypofractionated vs. conventional whole-breast irradiation: an objective, randomized multicenter assessment using spectrophotometry. *Radiother Oncol* 2020;146:172–179. https://doi.org/10.1016/j.radonc.2020.02.018.

[11] Russell NS, Knaken H, Bruinvis IAD, Hart AAM, Begg AC, Lebesque JV. Quantification of patient to patient variation of skin erythema developing as a response to radiotherapy. *Radiother Oncol* 1994;30:213–221. https://doi.org/10.1016/0167-8140(94)90460-X.

[12] Yamazaki H, Takenaka T, Aibe N, Suzuki G, Yoshida K, Nakamura S, *et al*. Comparison of radiation dermatitis between hypofractionated and conventionally fractionated postoperative radiotherapy: objective, longitudinal assessment of skin color. *Sci Rep* 2018;8:12306. https://doi.org/10.1038/s41598-018-30710-4.

[13] Yoshida K, Yamazaki H, Takenaka T, Tanaka E, Kotsuma T, Fujita Y, *et al*. Objective assessment of dermatitis following post-operative radiotherapy in patients with breast cancer treated with breast-conserving treatment. *Strahlenther Onkol* 2010;186:621–629. https://doi.org/10.1007/s00066-010-2134-1.

[14] Momm F, Bartelt S, Haigis K, Grosse-Sender A, Witucki G. Spectrophotometric skin measurements correlate with EORTC/RTOG-common toxicity criteria. *Strahlenther Onkol* 2005;181:392–395. https://doi.org/10.1007/s00066-005-1345-3.

[15] Bohner AMC, Koch D, Schmeel FC, Rohner F, Schoroth F, Sarria GR, *et al*. Objective evaluation of risk factors for radiation dermatitis in whole-breast irradiation using the spectrophotometric L*a*b color-space. *Cancers* 2020;12:2444. https://doi.org/10.3390/cancers12092444.

[16] Partl R, Jonko B, Schnidar S, Schollhammer M, Bauer M, Singh S, *et al*. 128 Shades of Red: objective remote assessment of radiation dermatitis by augmented digital skin imaging. *Stud Health Technol Inform* 2017;236:363–374. https://doi.org/10.3233/978-1-61499-759-7-363.

[17] Ranjan R, Partl R, Erhart R, Kurup N, Schnidar H. The mathematics of erythema: development of machine learning models for artificial intelligence assisted measurement and severity scoring of radiation induced dermatitis. *Comput Biol Med* 2021;139:104952. https://doi.org/10.1016/j.compbiomed.2021.104952.

[18] Pastore F, Conson M, D'Avino V, Palma G, Liuzzi R, Solla R, *et al*. Dose-surface analysis for prediction of severe acute radio-induced skin toxicity in breast cancer patients. *Acta Oncol* 2016;55:466–473. https://doi.org/10.3109/0284186X.2015.1110253.

[19] Yanagi T, Kamada T, Tsuji H, Imai R, Serizawa I, Tsujii H. Dose–volume histogram and dose–surface histogram analysis for skin reactions to carbon ion radiotherapy for bone and soft tissue sarcoma. *Radiother Oncol* 2010;95:60–65. https://doi.org/10.1016/j.radonc.2009.08.041.

[20] Kawamura M, Yoshimura M, Asada H, Nakamura M, Matsuo Y, Mizowaki T. A scoring system predicting acute radiation dermatitis in patients with head and neck cancer treated with intensity-modulated radiotherapy. *Radiat Oncol* 2019;14:14. https://doi.org/10.1186/s13014-019-1215-2.

[21] Takenaka T, Yamazaki H, Suzuki G, Aibe N, Masui K, Shimizu D, *et al*. Correlation between dosimetric parameters and acute dermatitis of post-operative radiotherapy in breast cancer patients. *Vivo* 2018;32:1499–1504. https://doi.org/10.21873/invivo.11406.

[22] Intel. Intel RealSense D435i, https://www.intelrealsense.com/depth-camera-d435i/ 2020. [Accessed 28 September 2020].

[23] Partl R, Lehner J, Winkler P, Kapp KS. Testing the feasibility of augmented digital skin imaging to objectively compare the efficacy of topical treatments for radiodermatitis. *PLoS One* 2019;14:e0218018. https://doi.org/10.1371/journal.pone.0218018.

[24] McLaren K. XIII—the development of the CIE 1976 (L* a* b*) uniform colour space and colour-difference formula. *J Soc Dyers Colourists* 1976;92:338–341. https://doi.org/10.1111/j.1478-4408.1976.tb03301.x.

[25] Park Y-I, Choi SH, Hong C-S, Cho M-S, Son J, Jang JW, *et al*. A pilot study of a novel method to visualize three-dimensional dose distribution on skin surface images to evaluate radiation dermatitis. *Sci Rep* 2022;12:2729. https://doi.org/10.1038/s41598-022-06713-7.

[26] Borm KJ, Loos M, Oechsner M, Mayinger MC, Paepke D, Kiechle MB, *et al*. Acute radiodermatitis in modern adjuvant 3D conformal radiotherapy for breast cancer - the impact of dose distribution and patient related factors. *Radiat Oncol* 2018;13:218. https://doi.org/10.1186/s13014-018-1160-5.

[27] Chen L-C, Papandreou G, Schroff F, Adam H. *Rethinking atrous convolution for semantic image segmentation*. arXiv; 2017. https://doi.org/10.48550/arXiv.1706.05587. Preprint arXiv: 170605587.

[28] Teichmann MT, Cipolla R. *Convolutional CRFs for semantic segmentation*. arXiv; 2018. https://doi.org/10.48550/arXiv.1805.04777. Preprint arXiv:180504777.

[29] Sudre CH, Li W, Vercauteren T, Ourselin S, Cardoso MJ. *Generalised dice overlap as a deep learning loss function for highly unbalanced segmentations*. arXiv; 2017. https://doi.org/10.1007/978-3-319-67558-9_28. 170703237.

[30] Kingma DP, Ba J. *Adam: a method for stochastic optimization*. arXiv; 2014. https://doi.org/10.48550/arXiv.1412.6980. Preprint arXiv:14126980.

[31] Kitajima M, Mikami K, Noto Y, Itaki C, Fukushi Y, Hirota Y, *et al*. Quantitative assessment of radiodermatitis through a non-invasive objective procedure in patients with breast cancer. *Mol Clin Oncol* 2020;12:89–93. https://doi.org/10.3892/mco.2019.1948.

[32] Sekine H, Kijima Y, Kobayashi M, Itami J, Takahashi K, Igaki H, *et al*. Non-invasive quantitative measures of qualitative grading effectiveness as the indices of acute radiation dermatitis in breast cancer patients. *Breast Cancer* 2020;27:861–870. https://doi.org/10.1007/s12282-020-01082-3.

[33] Yamazaki H, Yoshida K, Kotsuma T, Kuriyama K, Masuda N, Nishimura T, *et al*. Longitudinal practical measurement of

skin color and moisture during and after breast-conserving therapy: influence of neoadjuvant systemic therapy. *Jpn J Radiol* 2009;27:309–315. https://doi.org/10.1007/s11604-009-0345-0.

[34] Maillot O, Leduc N, Atallah V, Escarmant P, Petit A, Belhomme S, *et al*. Evaluation of acute skin toxicity of breast radiotherapy using thermography: results of a prospective single-centre trial. *Cancer Radiother* 2018;22:205–210. https://doi.org/10.1016/j.canrad.2017.10.007.

[35] Gonzalez Sanchis A, Brualla Gonzalez L, Sanchez Carazo JL, Gordo Partearroyo JC, Esteve Martinez A, Vicedo Gonzalez A, *et al*. Evaluation of acute skin toxicity in breast radiotherapy with a new quantitative approach. *Radiother Oncol* 2017;122:54–59. https://doi.org/10.1016/j.radonc.2016.09.019.

[36] Wada K, Watanabe M, Shinchi M, Noguchi K, Mukoyoshi T, Matsuyama M, *et al*. A study on radiation dermatitis grading support system based on deep learning by hybrid generation method. *Nihon Hoshasen Gijutsu Gakkai Zasshi* 2021;77:787–794. https://doi.org/10.6009/jjrt.2021_JSRT_77.8.787.

[37] Marks LB, Yorke ED, Jackson A, Ten Haken RK, Constine LS, Eisbruch A, *et al*. Use of normal tissue complication probability models in the clinic. *Int J Radiat Oncol Biol Phys* 2010;76:S10–S19. https://doi.org/10.1016/j.ijrobp.2009.07.1754.

[38] Pedersen J, Flampouri S, Bryant C, Liang X, Mendenhall N, Li Z, *et al*. Cross-modality applicability of rectal normal tissue complication probability models from photon- to proton-based radiotherapy. *Radiother Oncol* 2020;142:253–260. https://doi.org/10.1016/j.radonc.2019.09.017.

[39] Palma G, Monti S, Conson M, Xu T, Hahn S, Durante M, *et al*. NTCP models for severe radiation induced dermatitis after IMRT or proton therapy for thoracic cancer patients. *Front Oncol* 2020;10:344. https://doi.org/10.3389/fonc.2020.00344.

[40] Palma G, Monti S, Conson M, Pacelli R, Cella L. Normal tissue complication probability (NTCP) models for modern radiation therapy. *Semin Oncol* 2019;46:210–218. https://doi.org/10.1053/j.seminoncol.2019.07.006.

[41] Sun L-M, Huang E-Y, Liang J-A, Meng F-Y, Chang G-H, Tsao M-J. Evaluation the consistency of location of moist desquamation and skin high dose area for breast cancer patients receiving adjuvant radiotherapy after breast conservative surgery. *Radiat Oncol* 2013;8:50. https://doi.org/10.1186/1748-717X-8-50.

[42] Chyad MA, Alsattar HA, Zaidan BB, Zaidan AA, Al Shafeey GA. The landscape of research on skin detectors: coherent taxonomy, open challenges, motivations, recommendations and statistical analysis, future directions. *IEEE Access* 2019;7:106536–106575. https://doi.org/10.1109/access.2019.2924989.

[43] Ronneberger O, Fischer P, Brox T. U-net: convolutional networks for biomedical image segmentation. In: *International Conference on Medical Image Computing and Computer-assisted Intervention*. Springer; 2015. Available at: https://doi.org/10.48550/arXiv.1505.04597.

[44] Yakubovskiy P. Segmentation models Pytorch. GitHub repository. Available at: https://github.com/qubvel/segmentation_models.pytorch 2020. [Accessed 30 May 2022].